HHS Public Access

Author manuscript

Nat Neurosci. Author manuscript; available in PMC 2013 May 01.

Published in final edited form as:

Nat Neurosci. 2012 November ; 15(11): 1547–1555. doi:10.1038/nn.3239.

Lack of GPR88 enhances medium spiny neuron activity and alters motor- and cue-dependent behaviors

Albert Quintana[1], **Elisenda Sanz**[2], **Wengang Wang**[3], **Granville P. Storey**[3], **Ali D. Güler**[1], **Matthew J. Wanat**[2,4], **Bryan A. Roller**[1], **Anna La Torre**[5], **Paul S. Amieux**[2], **G. Stanley McKnight**[2], **Nigel S. Bamford**[3,6], and **Richard D. Palmiter**[1,*]

[1]Howard Hughes Medical Institute and Department of Biochemistry, University of Washington, Seattle, WA 98195

[2]Department of Pharmacology, University of Washington, Seattle, WA 98195

[3]Department of Neurology, University of Washington, Seattle, WA 98195

[4]Department of Psychiatry & Behavioral Sciences, University of Washington, Seattle, WA 98195

[5]Department of Biological Structure, University of Washington, Seattle, WA 98195

[6]Departments of Pediatrics, Psychology, the Graduate Program in Neurobiology and Behavior, and Center on Human Development and Disability, University of Washington and Seattle Children's Hospital, Seattle, WA 98105

Abstract

The striatum regulates motor control, reward, and learning. Abnormal function of striatal GABAergic medium spiny neurons (MSNs) is believed to contribute to the deficits in these processes that are observed in many neuropsychiatric diseases. The orphan G-protein-coupled receptor (GPCR) GPR88 is robustly expressed in MSNs and regulated by neuropharmacological drugs, but its contribution to MSN physiology and behavior is unclear. Here we show that in the absence of GPR88, MSNs have increased glutamatergic excitation and reduced GABAergic inhibition that together promote enhanced firing rates *in vivo*, resulting in hyperactivity, poor motor-coordination, and impaired cue-based learning in mice. Targeted viral expression of GPR88 in MSNs rescues the molecular and electrophysiological properties and normalizes behavior, suggesting that aberrant MSN activation in the absence of GPR88 underlies behavioral deficits and its dysfunction may contribute to behaviors observed in neuropsychiatric disease.

*Corresponding author: 1959 NE Pacific St. HHMI, University of Washington. Department of Biochemistry. Box 357370. Seattle, WA 98195. USA. palmiter@uw.edu.

AUTHOR CONTRIBUTIONS

A.Q. and R.D.P. designed the research. R.D.P. generated the *Gpr88*$^{Cre/Cre}$ mice. A.Q. performed the histological experiments. A.Q. and E.S. performed the RiboTag and biochemical experiments. E.S. performed and A.Q. analyzed the microarray experiment. W.W., G.P.S., and M.J.W. performed and analyzed the *in vitro* electrophysiological studies. A.Q. and A.D.G. performed and A.D.G. analyzed the *in vivo* electrophysiological experiments. A.Q. and B.A.R. performed and analyzed the behavioral experiments. A.Q. made the viral vectors and performed stereotaxic surgery. A.L. performed the neuronal primary culture experiments. P.S.A. and G.S.M. supervised the biochemical studies. N.S.B. supervised the electrophysiological studies. R.D.P. supervised the research. A.Q., N.S.B., and R.D.P. wrote the manuscript.

The striatum is a major component of the basal ganglia circuitry; it receives excitatory cortical and thalamic glutamatergic inputs and modulatory dopaminergic input, which together with inhibitory inputs from interneurons, are integrated and relayed to other basal ganglia components via GABAergic MSNs. MSNs express either D1- or D2-dopamine receptors (D1R and D2R), constituting the striatonigral (direct) and striatopallidal (indirect) pathways[1].

The pathophysiology of neurological disorders including Parkinson's, Huntington's, bipolar disorder, schizophrenia, and ADHD[2–5] are thought to involve altered basal ganglia function[1,2,6,7]. Although the roles of glutamatergic and dopaminergic neurons have been extensively characterized, there is still uncertainty about the causal mechanisms of these diseases, highlighting the importance of elucidating the underlying cellular mechanisms.

GPR88 is an orphan GPCR that is abundant in both D1R- and D2R-expressing MSNs[8]. *Gpr88* gene expression is modified by several anti-depressant therapies and pharmacological interventions[9–11] and induced both by glutamate and dopamine[8,12]. GPR88 deficiency alters sensory-motor gating, suggesting a role in neuropsychiatric diseases[12]. However, its intracellular signaling mechanisms and effects on MSN function are unknown. Here we show that the absence of GPR88 increases MSN excitability by modulating RGS4-dependent GABA and glutamatergic signaling, impairing motor- and cue-based behaviors, which can be restored by striatal GPR88 re-expression, underscoring the importance of GPR88 for normal striatal function.

RESULTS

Gpr88 is highly expressed in striatal MSNs

Mice with the *Gpr88* coding region replaced by a cassette encoding a Cre recombinase-EGFP fusion protein (Gpr88-Cre-EGFP; Methods and Fig. 1a) were made by gene targeting. When the Gpr88-Cre-EGFP mice were crossed with Cre-dependent reporter mice[13], expression of TdTomato marked all cells where Cre had been expressed, while EGFP revealed where Cre was currently being expressed. TdTomato labeling was abundant in the striatum (Fig. 1b); it filled projections to the substantia nigra pars reticulata (SNr) and external globus pallidus (GPe), indicating that both direct and indirect striatal MSNs express GPR88 (Fig. 1b). Some TdTomato-expressing cells were visible in other brain regions (Fig. 1b and Supplementary Table 1).

Expression of *Gpr88* in the adult brain was more restricted; EGFP-positive cells were readily observed in the striatum and olfactory tubercle (Fig. 1c). Regions of lower *Gpr88* expression were identified by immunohistochemistry against EGFP, which revealed *Gpr88* expression in cortex, thalamus, and inferior olive (Fig. 1d–g). There were fewer cortical EGFP-positive cells than TdTomato-positive cells indicating that *Gpr88* is expressed during development and silenced later.

Striatal *Gpr88* expression is confined to MSNs

To determine which striatal neurons express Gpr88-Cre-EGFP, the mice were bred with RiboTag mice[14] that allow Cre-dependent expression of HA-tagged ribosomal protein L22.

The HA tag enables immunoprecipitation of polysomes and associated mRNAs from cells that express Cre. We compared the relative abundance of transcripts in the pellets and the total tissue RNA (input) by qRT-PCR from striatum. *Gpr88* mRNA was enriched 4-fold in the pellets compared to the input (Fig. 1h; $t_{(4)}$=4.81, p<0.01 versus pellet, Student's t-test, two-tailed), confirming immunoprecipitation of polysomes from *Grp88*-expressing cells. There was comparable enrichment of the MSN-specific DARPP32 (*Pp1r1b)* Met-enkephalin (*Penk*), and dynorphin (*Pdyn*) transcripts, indicating that both D1R- and D2R-bearing MSNs express *Gpr88* (Fig. 1h; p<0.01 versus pellet, Student's t-test, two-tailed, $t_{(4)}$=12.02; $t_{(4)}$=4.84; $t_{(4)}$=6.18, respectively). In contrast, the expression of the interneuron-specific genes somatostatin (*Sst*), calretinin (*Calb2*), parvalbumin (*Parv*), and choline acetyl transferase (*Chat*) were de-enriched (Fig. 1h; p<0.001 versus pellet, Student's t-test, two-tailed, $t_{(4)}$=25.58; $t_{(4)}$=23.63; $t_{(4)}$=83.17; $t_{(4)}$=88.86, respectively), and all HA-positive cells co-localized with nuclear EGFP (Fig. 1h). Dynorphin immunofluorescence (marker for direct pathway MSNs) showed staining in a subset of the EGFP-positive cells (Fig. 1i). These results indicate that striatal *Gpr88* expression is restricted to MSNs.

To evaluate the role of *Gpr88* in MSN physiology, homozygous (*Gpr88*$^{Cre/Cre}$; *Gpr88* knockout mice) were generated. *Gpr88* expression, assessed by qRT-PCR, was absent in the striatum of *Gpr88*$^{Cre/Cre}$ mice compared to *Gpr88*$^{+/+}$ mice; *Gpr88*$^{Cre/+}$ mice had half as much *Gpr88* mRNA as *Gpr88*$^{+/+}$ mice (Fig. 1j; $F_{(2,9)}$=248.3, p<0.001, genotype, one-way ANOVA, SNK post-test). *Gpr88* deficiency had no apparent effect on striatal cell populations (Supplementary Fig. 1).

Altered behavior of *Gpr88*$^{Cre/Cre}$ mice

To elucidate the role of GPR88 in basal locomotor activity, mice were placed in activity chambers for 48 h. Activity during the first few hours, which reflects the response to novelty, was higher in *Gpr88*$^{Cre/Cre}$ mice (Fig. 2a; $t_{(18)}$=3.988, p<0.001, Student's t-test, two-tailed). All animals increased their activity during the nocturnal cycle and this response was greater in *Gpr88*$^{Cre/Cre}$ mice (Fig. 2a,b; $F_{(1,18)}$=4.90, p<0.05, genotype, repeated-measures (rm) ANOVA, Bonferroni post-test); daytime activities were comparable.

Motor coordination and balance were assessed using a rotarod; mice were placed on top of an accelerating rod and the latency to fall was scored. While *Gpr88*$^{+/+}$ mice improved their performance with each experimental session (Fig. 2c; $F_{(2,14)}$=6.566, p<0.001, time, one-way ANOVA) *Gpr88*$^{Cre/Cre}$ mice fell more quickly and showed no improvement with training (Fig. 2c; $F_{(1,27)}$=32.70, p<0.001, genotype, rmANOVA, SNK post-test). The latency to fall from an inverted wire mesh was shorter for *Gpr88*$^{Cre/Cre}$ (n=13) mice compared to *Gpr88*$^{+/+}$ (n=15) mice (133.70±12.65 *Gpr88*$^{+/+}$ versus 62.83±12.52 *Gpr88*$^{Cre/Cre}$, $t_{(26)}$=3.957, p<0.001, mean ± s.e.m, Student's t-test, two- tailed), confirming impairments in motor coordination or strength of *Gpr88*$^{Cre/Cre}$ mice.

Mastery of the Morris water maze requires intact striatal function[15,16]. *Gpr88*$^{Cre/Cre}$ mice had longer latencies to find the platform compared to *Gpr88*$^{+/+}$ during the first 4 training sessions (Fig. 3a, sessions 1–4; $F_{(1,19)}$=6.06, p<0.05, genotype, rmANOVA); however, with more training the latencies between genotypes were equivalent (Fig. 3a, sessions 6–9). Probe trials showed that both *Gpr88*$^{+/+}$ and *Gpr88*$^{Cre/Cre}$ mice preferred the quadrant where the

platform had been hidden (Fig. 3b,c; $F_{(3,57)}$=15.88 (probe1) and $F_{(3,57)}$=58.65 (probe 2), p<0.001, quadrant, rmANOVA, Bonferroni post-test). *Gpr88*$^{Cre/Cre}$ and *Gpr88*$^{+/+}$ mice had the same swim speed (Supplementary Fig. 2a,b). Hence, *Gpr88*$^{Cre/Cre}$ had mild impairment in initial performance of the task but visuospatial memory and learning were intact.

Associative learning depends on intact striatal function[17]. We tested the ability of the mice to learn the position of an escape platform in a water-based, U-maze paradigm[18] (Fig. 3d). *Gpr88*$^{+/+}$ and *Gpr88*$^{Cre/Cre}$ mice were trained daily for three days to learn a turn-based strategy to find a platform placed at the end of one maze arm. The percentage of correct choices was the same between genotypes (Fig. 3d), although *Gpr88*$^{Cre/Cre}$ mice had higher latencies to reach the decision point and platform (Supplementary Fig. 2c,d). Animals were then forced to shift from the turn-based to a cue-based strategy, in which the platform was associated to the color of the arms for seven more daily sessions. After the shift, the number of correct choices decreased and then improved with further training; *Gpr88*$^{+/+}$ mice reached >90% correct choices after 4 d but *Gpr88*$^{Cre/Cre}$ mice were slower to learn the new escape strategy (Fig. 3d; $F_{(1,19)}$=4.39, p<0.05, genotype, rmANOVA, Bonferroni post-test) and had higher latencies to reach the platform (Supplementary Fig. 2d). We tested a second cohort of mice exclusively in the cue-based, U-water maze for 5 d. *Gpr88*$^{Cre/Cre}$ mice were slower to learn the task (Fig. 3e; $F_{(1,12)}$=6.70, p<0.05, genotype, rmANOVA, Bonferroni post-test), indicating impaired cue-based learning.

Mice were also tested in a 2-way active avoidance paradigm. Performance in this task depends on striatal integrity, being affected by neuropsychiatric drugs and striatal lesions[17,19]. Mice learn that a sound cue predicts a foot-shock and avoid the shock by moving to the other side of the box. Mice were trained with 100 trials per day for 5 d and the percentage of avoidance responses was measured. Acquisition of this task was impaired in *Gpr88*$^{Cre/Cre}$ relative to *Gpr88*$^{+/+}$ mice (Fig. 3f; $F_{(1,22)}$=11.07, p<0.05; genotype, rmANOVA, Bonferroni post-test). Both the latencies to escape after the foot shock or the sound cue during the first 10 trials (when neither group had mastered the task) were not different (Supplementary Fig. 2e,f), suggesting that the impaired acquisition of the task by *Gpr88*$^{Cre/Cre}$ mice is not attributable to decreased pain sensitivity or motor deficits. These combined results indicate that *Gpr88*$^{Cre/Cre}$ mice have deficits in the acquisition and integration of visual or auditory cues leading to impaired performance of these behavioral tasks.

Enhanced firing rate of MSNs of *Gpr88*$^{Cre/Cre}$ mice *in vivo*

To determine if absence of GPR88 affected MSN activity, we recorded freely moving *Gpr88*$^{+/+}$ and *Gpr88*$^{Cre/Cre}$ mice with chronically implanted electrodes in the dorsal (predominantly dorsomedial) striatum, a region controlling initiation and acquiring of goal-directed behaviors[3] and cognitive flexibility[18] (Supplementary Fig. 3a). Mice were habituated to the recording environment for one week at which point basal locomotion and rearing activity were comparable Supplementary Fig. 3b,*c*). Putative MSNs (n=70 cells *Gpr88*$^{+/+}$, n=52 cells *Gpr88*$^{Cre/Cre}$, 6 mice per group), identified as units having >300-μs valley width as described[20], had similar waveform properties between the two groups (Fig. 4a and Supplementary Fig. 3d,e; valley width 484 ± 10 *Gpr88*$^{+/+}$ versus 480 ± 10

Gpr88$^{Cre/Cre}$, mean ± s.e.m, p>0.05 Student's t-test, two-tailed; peak amplitude 14,193 ± 4485 *Gpr88*$^{+/+}$ versus 14,050 ± 5760 *Gpr88*$^{Cre/Cre}$; mean ± s.e.m, p>0.05 Student's t-test, two-tailed). MSNs from *Gpr88*$^{Cre/Cre}$ mice had a higher average firing rate than from *Gpr88*$^{+/+}$ mice (Fig. 4b; $t_{(119)}$=2.096, p<0.05 versus *Gpr88*$^{+/+}$, Student's t-test, two-tailed).

MSNs transition between a relatively depolarized "up-state", where most action potentials occur, and a less active, hyperpolarized "down-state"[21]. Analysis of MSN activity revealed two populations; one with a firing pattern characterized by a highly variable inter-spike intervals (ISI), which corresponded to bursts of activity intermingled with pauses with few spikes and a second population with reduced ISI variability, indicative of continuous firing (Fig. 4c). A higher percentage of MSNs from *Gpr88*$^{Cre/Cre}$ mice showed continuous firing (44.28% *Gpr88*$^{+/+}$ versus 61.53% *Gpr88*$^{Cre/Cre}$ cells; p<0.05, Fisher's exact test), suggesting that the MSNs from *Gpr88*$^{Cre/Cre}$ mice are more excitable (Fig. 4d).

Altered neurotransmitter signaling in *Gpr88*$^{Cre/Cre}$ MSNs

To determine how the absence of GPR88 increases striatal excitability, whole-cell, patch-clamp recordings were obtained from dorsal MSNs in striatal slices. Current-clamp recordings revealed inward rectification following depolarizing current pulses and equivalent resting membrane potentials in cells from *Gpr88*$^{+/+}$ and *Gpr88*$^{Cre/Cre}$ (−71.56±0.25 mV for *Gpr88*$^{+/+}$ versus −71.38±0.23 mV for *Gpr88*$^{Cre/Cre}$; mean±s.e.m, n=14 cells each; p>0.05, Student's T-test, two-tailed), but input resistance was increased in *Gpr88*$^{Cre/Cre}$ cells (Fig. 5a; 22.90±2.28 MΩ for *Gpr88*$^{+/+}$ versus 34.78±4.9 MΩ for *Gpr88*$^{Cre/Cre}$; mean±s.e.m, n=16–18 cells; $t_{(31)}$=0.02, p<0.05, Student's t-test, two-tailed). Enhanced input resistance in MSNs suggested alterations in synaptic drive because it was not due to inwardly-rectifying K^+ currents[22] (Supplementary Fig. 4a,b).

Baseline tonic GABA currents in MSNs from *Gpr88*$^{Cre/Cre}$ mice were reduced. The $GABA_A$ receptor antagonist bicuculline (10 μM) provoked a smaller change in the holding current [$t_{(16)}$=3.39, p<0.01] and root mean square noise in *Gpr88*$^{Cre/Cre}$ cells (Fig. 5b,c; $t_{(16)}$=2.26, p<0.05, Student's t-test, two-tailed). Furthermore, $GABA_A$ receptor- mediated currents in *Gpr88*$^{Cre/Cre}$ cells were less responsive to bath-applied GABA (Fig. 5d; $t_{(16)}$=2.12, p<0.05, Student's t-test, two-tailed). In response to local intrastriatal stimulation (in the presence of glutamate and dopamine receptor antagonists), the peak evoked inhibitory post-synaptic currents (eIPSCs) were suppressed in MSNs from *Gpr88*$^{Cre/Cre}$ mice (Fig. 5e,f; $F_{(9, 225)}$=6.04, p<0.05, genotype, two-way ANOVA, Bonferroni post-test) and the mean stimulation current required to evoke an IPSC in MSNs was higher in cells from *Gpr88*$^{Cre/Cre}$ mice (Fig. 5f; t(30)= −2.18, p<0.05, Student's t-test, two-tailed).

To assess changes in glutamatergic signaling, excitatory postsynaptic currents (EPSCs) were measured in MSNs in response to cortical stimulation. The mean peak response amplitudes were greater in cells from *Gpr88*$^{Cre/Cre}$ mice at stimulation intensities >0.6 mA (Fig. 5g,h; $F_{(9, 90)}$=4.40, p<0.05, 2-way ANOVA, Bonferroni post-test) and the stimulation threshold required to evoke an EPSC was lower in MSNs from *Gpr88*$^{Cre/Cre}$ (Fig. 5h; $t_{(34)}$=2.82, p<0.01, Student's t-test, two-tailed).

D1R- and D2R-containing MSNs differ in their electrophysiological properties and their contributions to animal behavior[23–26]. We took advantage of the segregation of the direct and indirect pathway projections to label D1R- and DR2-expressing MSNs[1] by injecting retrogradely transported, fluorescent latex beads into the SNr or the GPe of *Gpr88*$^{Cre/Cre}$ mice (Supplementary Fig. 4c). No differences were observed in response to cortical excitatory input or the tonic GABA currents in whole-cell, patch-clamp recordings in D1R or D2R MSNs from striatal slices (Supplementary Fig. 4d–f), suggesting that both populations are affected by GPR88 deficiency. We evaluated the D1R- and D2R-mediated responses *in vivo* by analyzing the locomotor response to amphetamine. *Gpr88*$^{Cre/Cre}$ mice had greater locomotion response after exposure to repeated doses of amphetamine (2.5 mg/kg) compared to *Gpr88*$^{+/+}$ mice (Supplementary Fig. 4g; $F_{(1,8)}$=9.80, p<0.05, genotype, rmANOVA). To tease apart the contribution of each MSN subpopulation, varying concentrations of a D1R (SKF-81297) or a D2R (quinpirole) agonist were administered. SKF-82197 increased locomotion more in *Gpr88*$^{+/+}$ mice than in *Gpr88*$^{Cre/Cre}$ mice (Supplementary Fig. 4h; $F_{(1,10)}$=9.18, p<0.05, genotype, rmANOVA), whereas quinpirole reduced locomotion in *Gpr88*$^{+/+}$ mice but increased locomotion in *Gpr88*$^{Cre/Cre}$ mice (Supplementary Fig. 4i; $F_{(1,9)}$=49.91, p<0.05, genotype, rmANOVA).

Striatal mRNA and neurotransmitter content in *Gpr88*$^{Cre/Cre}$ mice

To determine if the increased activity of MSNs in *Gpr88*$^{Cre/Cre}$ mice involves alterations in neurotransmitter levels, we measured amino acids and their neurotransmitter-related metabolites in *Gpr88*$^{+/+}$ and *Gpr88*$^{Cre/Cre}$ striatal punches by HPLC. No differences were detected in the levels of dopamine, norepinephrine or serotonin. (Supplementary Table 2).

Microarray analysis of mRNA abundance in striatal punches from *Gpr88*$^{+/+}$ and *Gpr88*$^{Cre/Cre}$ mice coupled with a gene ontology analysis showed that the most of the over-represented mRNAs corresponded to negative regulation of cell communication (Supplementary Table 3a), confirming an inhibitory role of GPR88. Of this list, 50 mRNAs were down-regulated and 39 were up-regulated in *Gpr88*$^{Cre/Cre}$ mice compared to *Gpr88*$^{+/+}$ mice by >1.35 fold (Supplementary Table 3b,c), including genes associated with striatal disorders, such as *Adss*[27], *Fbxl21*[28] and *Rgs4*[29] (Supplementary Table 3b,c). We used qRT-PCR to measure mRNA levels from genes encoding neurotransmitter receptors, namely dopaminergic (*Drd1*, *Drd2*), glutamatergic (*Grin1, Grin2a, Grin2b, Grm1, Grm2, Grm3, Grm5*) and GABAergic (*Gababr1, Gababr2, Gabrb1, Gabrb3, Gad1*), neuropeptides (*Pdyn, Penk),* and molecules involved in intracellular signaling (*Ppp1r1b*, *Rgs4*) in whole striata from *Gpr88*$^{+/+}$ and *Gpr88*$^{Cre/Cre}$ mice (Fig. 6a). Among these mRNAs, only *Rgs*4 mRNA was significantly reduced in *Gpr88*$^{Cre/Cre}$ mice (Fig. 6a, $t_{(6)}$=5.417, p<0.01 versus *Gpr88*$^{+/+}$, Student's t-test, two-tailed). Regulator of G-protein signaling 4 (RGS4) is a GTPase-activating protein involved in the regulation of Gαi and Gαq GPCRs[30] that has been linked to schizophrenia and motor deficits[29,31–33].

Changes in GluR1 and GABA receptors in *Gpr88*$^{Cre/Cre}$ mice

Alterations in RGS4 mRNA suggested abnormal Gαi/Gαq GPCR signaling and potentially changes in receptor phosphorylation. Western blot analysis of the phosphorylation at serine 897 (S897) of NR1, the essential subunit of NMDA glutamate receptor, and at serines 831

and 845 (S831, S845) of GluR1, a subunit of the AMPA glutamate receptor was performed. PKA/PKC-dependent S831 and S845 phosphorylation of GluR1 (pGluR1) was increased in *Gpr88*$^{Cre/Cre}$ mice, which facilitates AMPA receptor signaling[34] ($t_{(4)}$=9.72, p<0.001(S845) and $t_{(4)}$=6.45, p<0.01(S831), Student's t-test, two-tailed); but pNR1 phosphorylation was unchanged. The total amount of GluR1, NR1, and the synaptic protein PSD95 were the same in *Gpr88*$^{+/+}$ and *Gpr88*$^{Cre/Cre}$ mice (Fig. 6b,c).

Western blot analysis showed that the β1 subunit of the $GABA_A$ receptor was unaltered, but the β3 protein was reduced in striata of *Gpr88*$^{Cre/Cre}$ mice (Fig. 6b,c; $t_{(4)}$=6.016, p<0.01, Student's t-test, two-tailed and Supplementary Fig. 5), despite normal mRNA levels, suggesting post-translational regulation[35]. The β3 subunit is required for normal tonic $GABA_A$ receptor currents in MSNs[36], suggesting that alterations in receptor abundance/phosphorylation may account for some of the electrophysiological observations.

Striatal Gpr88 re-expression rescues mutant phenotype

To confirm the contribution of striatal GPR88 expression to the phenotype of *Gpr88*$^{Cre/Cre}$ mice, we produced an adeno-associated virus (AAV) encoding a human GPR88-TdTomato fusion protein (Supplementary Fig. 6a). Transduction of primary neuronal cultures showed targeting of the Gpr88-TdTomato protein to the membrane (Supplementary Fig. 6b,c), colocalization with postsynaptic protein PSD95 and proximity to presynaptic boutons (Supplementary Fig. 6b,c), suggesting targeting to dendritic spines, in agreement with previous observations using an antibody against GPR88[8].

To rescue the behavioral phenotype, a Cre-dependent version of the virus (Fig. 7a) was injected at multiple coordinates in *Gpr88*$^{Cre/Cre}$ mice to achieve maximum striatal coverage (virally rescued *Gpr88*$^{Cre/Cre}$ mice, VR-KO mice). As a control, an AAV vector expressing only TdTomato (Fig. 7b) was injected in *Gpr88*$^{+/+}$ mice (Sham-WT) and *Gpr88*$^{Cre/Cre}$ mice (Sham-KO). By measuring immunofluorescence of TdTomato, ~45% of total striatal area was transduced in the VR-KO mice (Fig. 7c and Supplementary Fig. 6d). Fluorescence was observed throughout soma and processes. Some transduced neurons allowed visualization of the fusion protein in dendritic spines (Fig. 7d). TdTomato-positive cells co-localized with nuclear EGFP, confirming MSN targeting (Fig. 7d).

Two weeks after AAV injection, we evaluated performance of mice in several motor/learning tests. Sham-KO and naïve-KO mice had similar responses, so those data were pooled. The locomotor activity of the VR-KO mice was the same as Sham-WT mice, and less than Sham KO mice (Fig. 7e;p<0.01, Kruskal-Wallis test, Dunn post-test). More demanding behaviors such as rotarod performance (Fig. 7f; $F_{(2,33)}$=12.04, p<0.05, one-way ANOVA, SNK post-hoc test) and 2-way active avoidance (Fig. 7g; $F_{(2,20)}$=4.70, p<0.05, genotype, rmANOVA, Bonferroni post-test) were also restored to normal in the VR-KO mice (Fig. 7 f,g). Expression of *Gpr88* mRNA in striatum of VR-KO mice was confirmed by qRT-PCR with a set of primers designed to hybridize to both mouse (endogenous) and human (viral rescue) *Gpr88*. Similar levels of *Gpr88* expression were observed in VR-KO and Sham-WT mice (Fig. 7h; $F_{(2,11)}$=42.95, p<0.001, one-way ANOVA, SNK post-hoc test). Furthermore, both striatal pGluR1 S845 (Fig. 7i; $F_{(2,14)}$=5.58, p<0.05, one-way ANOVA, SNK post-test) and $GABA_A$ receptor β3 abundance (Fig. 7j; $F_{(2,14)}$=5.02, p<0.05,

one-way ANOVA, SNK post-test) were normalized in VR-KO mice, suggesting a direct link between GPR88 deficiency and the molecular alterations observed in KO mice.

We evaluated tonic GABA currents and evoked EPSCs by whole-cell, patch-clamp recordings from striatal slices obtained from Sham-KO and VR-KO mice. Compared to MSNs from Sham-KO mice, baseline tonic GABA currents (Fig. 8a; $t_{(16)}=2.37$, $p<0.05$, Student's t-test versus VR-KO) were increased, the mean peak excitatory response amplitudes were reduced (Fig. 8b; $F_{(9, 207)}=4.61$, $p<0.01$, genotype, 2-way ANOVA), and the cortical stimulation threshold required to evoke an EPSC was increased in VR-KO cells (Fig. 8c; $t_{(25)}=5.21$, $p<0.001$, Student's t-test), with values comparable to MSNs from *Gpr88*$^{+/+}$ mice (Fig. 5h). Dialysis of the RGS4 inhibitor CCG-63802 (100 μM)[33] via the recording electrode into MSNs from VR-KO mice decreased tonic GABA currents (Fig. 8a; $t_{(9)}=2.03$, $p<0.05$, Student's t-test, two-tailed) and increased mean peak excitatory response amplitudes (Fig. 8b; $F_{(9, 144)}=2.07$, $p<0.05$, genotype, 2-way ANOVA), while reducing the cortical stimulation threshold required to evoke an EPSC (Fig. 8c; $t_{(14)}=2.83$, $p<0.05$, Student's t-test, two-tailed); thus, mimicking the loss of GPR88 and implicating RGS4 in the altered properties of MSNs from *Gpr88*$^{Cre/Cre}$ mice.

DISCUSSION

Our results link the activity of GPR88 to normal striatal MSN function. We confirmed that *Gpr88* is highly expressed in the striatum, with expression limited to D1R- and D2R-containing MSNs. Inactivation of the *Gpr88* locus leads to increased glutamate receptor phosphorylation and altered $GABA_A$ receptor composition, which together enhance excitability in both D1R- and D2R-expressing MSNs *in vitro* and elevate MSN firing *in vivo*. The enhanced excitability of MSNs in *Gpr88*$^{Cre/Cre}$ mice results in behavioral hyperactivity, deficits in motor coordination, impaired acquisition, and integration of visual or auditory cues leading to poor performance in cue-based tasks. We restored electrophysiological responses, prevented hyperactivity and learning deficits in *Gpr88*$^{Cre/Cre}$ mice by re-expressing a human GPR88-TdTomato fusion protein in MSNs. Although we cannot rule out roles of GPR88 in other brain regions, the behavioral restoration observed after viral rescue demonstrates the importance of GPR88 function in the striatum.

GABA-induced responses in slices and tonic GABA conductance were reduced in MSNs of *Gpr88*$^{Cre/Cre}$ mice. These results are likely due to decreased $GABA_A$ receptor subunit β3 levels[37]. The tonic GABA input in MSNs is mediated by extra-synaptic (δ-and β3-expressing) $GABA_A$ receptors[38,39]. Lack of phospho-specific antibodies impeded determination of phosphorylation status of β3-subunit containing $GABA_A$ receptors, but they are regulated by PKA and PKC[35]. *Gpr88*$^{Cre/Cre}$ mice have less striatal RGS4, which promotes signaling by other Gαi- and Gαq-coupled GPCRs within MSNs[30], resulting in altered kinase activity and abnormal MSN excitability. Changes in kinase activity could mediate the increase in GluR1 phosphorylation observed in *Gpr88*$^{Cre/Cre}$ mice that underlies the increased AMPA receptor-mediated responses in *Gpr88*$^{Cre/Cre}$ mice. Accordingly, RGS4 inhibition was sufficient to abolish the restoration of the electrophysiological properties of MSNs after virally-mediated GPR88 re-expression. We propose that the absence of GPR88

modifies transcription and intracellular signaling leading to changes in RGS4 activity and increased MSN excitability.

The behavioral changes observed in *Gpr88*$^{Cre/Cre}$ mice resemble neurological disease processes associated with the striatum[3,5–7]. The *Gpr88*$^{Cre/Cre}$ mice learned response-based learning in the U maze but were slower to learn cue-based tasks, such as the Morris water maze, U maze and the two-way active avoidance. Burst-firing in dopamine neurons is thought to facilitate LTP and thereby contribute to cue-based learning through modulation of the signal-to-noise ratio in MSNs[40,41]. Therefore, the increased firing rate of MSNs in the *Gpr88*$^{Cre/Cre}$ mice may dampen the dynamic range of MSNs in response to burst firing by dopamine neurons and this could impair cue-based learning. We confirmed D2R agonist hypersensitivity in *Gpr88*$^{Cre/Cre}$ mice[12], and observed reduced D1R agonist effects in *Gpr88*$^{Cre/Cre}$ mice, suggesting altered dopaminergic signaling in both MSN populations of *Gpr88*$^{Cre/Cre}$ mice. While alterations in dopaminergic signaling have received the most attention in neurological disorders[5,42], our results illustrate that alterations in MSNs may also be involved.

Our findings suggest that tonic activation of MSNs in *Gpr88*$^{Cre/Cre}$ mice impairs integration and filtering of information in the striatum. Accordingly, *Gpr88*$^{Cre/Cre}$ mice have impaired pre-pulse inhibition (PPI; data not shown) as shown previously[12], an indicator of defective sensorimotor gating, that is observed after striatal lesions and found in many neuropsychiatric diseases[43–45]. Furthermore, administration of antidepressants[11,12], lithium[46] and valproate[47] change *Gpr88* expression, which may mediate some of the drug effects. It remains unclear how GPR88 is activated, as identification of its ligand has been elusive. Perhaps GPR88 functions without ligand activation; it may be regulated by altering the abundance of the protein rather than by a typical ligand-activation mechanism. Alternatively, MSN-specific chaperones/partners may be necessary for proper targeting/signaling of GPR88, which would preclude common high-throughput, heterologous-expression approaches. Regardless of these uncertainties, we show that GPR88 is important for the regulation of MSN excitability and that alteration in its function may contribute to the behavioral deficits caused by some neuropsychiatric diseases.

ONLINE METHODS

Animals

All animal experiments were approved by the Animal Care and Use Committee at the University of Washington. Group-housed, male and female C57Bl6/J (2–4 months old) mice were maintained with rodent diet (5053, Picolab, Hubbard, OR) and water available *ad libitum* with a 12-hr, light-dark cycle at 22°C.

Generation of RiboTag[16] and Rosa26-floxed stop-TdTomato (line Ai14)[13] mice have been described.

Generation of Gpr88-Cre mice

The 2-exon *Grp88* gene was subcloned from a C57Bl/6 BAC clone. Most of the open reading frame of *Gpr88* from just upstream of the initiation codon was replaced by a *Cre*-

EGFP cassette with a myc-tag and nuclear localization signal at the N-terminus. Both arms of the targeting construct were inserted into a targeting vector with frt-flanked *Sv-Neo* gene and *Pgk-DT$_A$* and *HSV-TK* genes and electroporated into C57Bl/6 embryonic stem cells; clones were screened by Southern blot (*Nco*1 digestion) using a unique probe 5′ of one arm. After germ-line transmission, the *Sv-Neo* gene was removed by breeding with FLPer mouse[48] and backcrossed to C57Bl/6 mice. Heterozygous (*Gpr88*$^{Cre/+}$) mice were bred to obtain mice homozygous for Cre (*Gpr88*$^{Cre/Cre}$*;Gpr88* knockout); heterozygous mice (*Gpr88*$^{Cre/+}$) and wild-type mice (*Gpr88*$^{+/+}$) at the expected Mendelian ratios. No differences were observed in body weight or lifespan between genotypes. Genotyping by PCR was performed with 2 different strategies (Supplementary Table 4).

Behavioral assays

Spontaneous locomotion was assessed in chambers (Columbus Instruments) with *ad libitum* access to food and water for 48 h. Distance traveled was calculated by Optomax software.

Rotarod was performed by placing the mice on an accelerating rod (4 to 40 rpm over the course of a 3-min trial, 3 trials/day, 20-min inter-trial interval (ITI), for three days)[49]. Latency to fall/fail to stay on top of the rod were recorded.

Hanging wire grip test was performed by placing mice on an inverted 15.5-cm wide wire grid 42 cm above a padded surface with a maximum trial time of 3 min[50] (3 trials, 15-min ITI). The average latency to fall were recorded.

The Water-U maze test is a metal, U-maze with arms (50 cm, one black and one white) bent back towards the stem (45 cm)[15]. An escape platform, not visible from end of stem, was present at the end of one of the two arms. Maze arms were alternated in a non-repetitive, pseudo-random sequence daily (10 trials/day, 3- to 5-min ITI)[18]. The percentage of correct trials and latencies to reach the platform (escape latencies) and the end of the stem (decision point) were recorded. Mice remained in the maze until a correct turn was made to ensure an equal number of reinforced responses. The strategy-shifting procedure consisted of two phases. For Phase 1, the mice had to learn a turn-based strategy for 3 d with the escape platform always on the same side of the ramp. For Phase 2 (days 4 through 7), the platform was associated to the arm color (cue-based strategy). For cue-based experiments, naïve mice were only trained in Phase 2 (5 days).

For the Morris water maze, mice were trained to locate a hidden platform over a period of 8 d (days 1–4 and 6–9) with four 90-s trials/day in a circular pool (84 cm diameter)[15]. On each trial, mice were released into the pool from a different location. Sessions were video-recorded and analyzed with EthoVision software (Noldus). Latency to reach the hidden platform and swim speed was recorded. On day 5 and 10, mice performed a no-platform 90-s spatial memory probe trial; the percentage of time spent in each quadrant was recorded.

In the two-way active avoidance test, mice were placed in a two-chamber apparatus (PACS-30 shuttle boxes, Columbus Instruments)[51]. Mice were exposed to a 2-s foot shock (0.3 mA, 3-min habituation), presented during the last 2 s of a 7-s tone (80 dB, 2.5 kHz). Mice could avoid the shock by Moving to the opposite side of the chamber during the 5-s

cue presentation. Mice were trained for 4 d (100 trials/d, 40-sec ITI). The percentage of shocks avoided per session was recorded.

All behavioral experiments were carried out in a blind and randomized manner.

Histology

Histology was performed as described[49]. Primary antibodies to HA (1:1000, Covance), Dyn (1:500, Santa Cruz), EGFP (1:1000, Invitrogen), TdTomato (1:500, Clontech) were used.

Striatal cell cultures

Brains were removed from 16-day C57BL/6J mouse embryos and striata were dissected in cold Hanks's balanced salt solution (Sigma). Striatal neurons were dissociated with a papain/DNase 1 solution (Worthington Biochemical) in serum-free medium for 5 min at 37°C and triturated 10 times with a Pasteur pipette. Dissociation was stopped with ovomucoid inhibitor/albumin and cells were centrifuged at 300 rcf for 3 min. Neurons were plated (2×10^5/well) on poly-D-lysine/laminin-coated coverslips (Sigma) in a 24-well culture dish and maintained for 7–12 days in serum-free Neurobasal medium (Gibco) supplemented with glutamine (2 mM), B27 (Gibco) and BDNF (20 μg/ml). Cells were fixed for 30 min in 4% paraformaldehyde and stained using an antibody to PSD95 (1:500, Zymed) and a pre-synaptic marker, Bassoon (1:500, Stressgen).

Microarrays

For microarray analysis, 150 ng of total RNA was amplified and biotin-labeled using the Illumina TotalPrep RNA Amplification kit (Ambion) and 750 ng of the labeled cRNA was hybridized to a MouseRef-8v2.0 gene expression BeadChip (Illumina). Signal was detected using the BeadArray Reader (Illumina) and analyzed using the GenomeStudio software (Illumina). Gene ontology (WebGestalt2 v1.1.974, Vanderbilt University)[52] was performed selecting genes with >1.2 fold difference in abundance and DiffScore>13 or $p<0.05$ (Illumina Custom test, Illumina GenomeStudio Software®); of these genes, those >1.35 fold are described in Supplementary Table 3. Raw data is accessible at http://www.ebi.ac.uk/arrayexpress/ (Accession# E-MTAB-1282).

Polysome immunoprecipitation and qRT-PCR

HA-tagged polysome immunoprecipitation and qRT-PCR analysis were performed as described[14]. RNA was isolated from total input and from anti-HA polysomes (pellet). All mRNAs were normalized to beta-actin (*Actb*) levels using the ΔΔCt method. The immunoprecipitated RNA samples were compared to the input sample in each case. For qRT-PCR, total RNA was isolated from dissected striata and normalized to *Actb* levels using the ΔΔCt method. Sequences of the primers used are available in Supplementary Table 4.

Western blot

Western blots for pGluR1 S845,S831 (1:5000, Cell Signaling), GluR1 (1:5000, Chemicon), pNR1 S897 (1:1000 Millipore), $GABA_A$ β1(1:1000, Abcam), $GABA_A$ β3 (1:750,

Millipore), PSD95 (1:500, Zymed) and β-actin (1:40000, Sigma) were performed as described[14].

Slice electrophysiology

Coronal brain slices (300 μm) were prepared using 4- to 8-wk-old male *Gpr88*$^{+/+}$ (n=21) and *Gpr88*$^{Cre/Cre}$ mice (n=22)[7]. For current clamp experiments, patch pipettes (4–6 MΩ) contained (in mM): 112 K-gluconate, 17.5 KCl, 4 NaCl, 1 $MgCl_2$, 0.5 $CaCl_2$, 5 MgATP, 5 EGTA, 10 HEPES, 1 Na-GTP, and 5 K_2-ATP (pH 7.2–7.3, 270–280 mOsm). For voltage clamp experiments, pipettes contained (in mM): 125 Cs-methanesulfonate, 3 KCl, 4 NaCl, 1 $MgCl_2$, 5 MgATP, 5 EGTA, 8 HEPES, 1 Tris-GTP, 10 di-sodium phosphocreatine, 0.1 leupeptin and QX-314. For tonic GABA currents, pipettes contained (in mM): 137 CsCl, 3 KCl, 4 NaCl, 1 $MgCl_2$, 10 HEPES, 10 EGTA, 12 phosphocreatine, 5 Na_2ATP, and 0.2 NaGTP. The mean holding current (recorded in the presence of (in μM): 10 NBQX, 50 APV, 40 CPCCOEt, and 10 MPEP) was determined at the peak value of a Gaussian fit of an all-points histogram obtained from two 30-s windows. I_{rms} was calculated by averaging sixty individual 50-ms epochs containing 250 amplitude measurements. Inwardly-rectifying K^+ currents were measured using voltage steps from −30 to −140 mV with the K^+-channel blocker Cs^+ (1 mM)[53,54]. Pipettes contained (in mM): 135 KMeSO4, 5 KCl, 0.5 CaCl2, 5 HEPES, 5 EGTA, 12 phosphocreatine, 2 Na2ATP, and 0.3 NaGTP. Voltage-dependent Na^+ and $Ca2^+$ conductances were blocked using 3 μM TTX and 100 μM $Cd2^+$, respectively. Maximal $GABA_A$ receptor-mediated currents during GABA application were recorded with (in μM): 100 APV, 10 CNQX, 1 strychnine, 0.1 eticlopride, and 10 CGP-52432 to block ionotropic glutamate, glycine, dopamine, and $GABA_B$ receptors, respectively. EPSCs and IPSCs in striatal MSNs were evoked by tungsten bipolar electrical stimulation of the dorsal cortex or striatum, respectively[26]. EPSCs were isolated by blocking $GABA_A$ receptors with bicuculline. IPSCs were isolated by blocking ionotropic and metabotropic glutamate and dopamine receptors with (in μM): 10 NBQX, 50 APV, 40 CPCCOEt, 10 MPEP, 10 SCH23390, and 10 sulpiride. Cells showing variable latencies or durations or those with series resistance greater than 20 MΩ or changing by >20% were rejected[7]. Analysis was performed using Clampfit (Molecular Devices).

Freely moving *in vivo* electrophysiology

Electrophysiological recordings in striatum of freely moving animals (n=6 per group) were obtained as described[40]. MSNs were identified as cells with valley widths greater than 300 μs[20]. Four-tetrode microdrives (Neuralynx) were implanted in the dorsal striatum of anesthetized mice (stereotaxic coordinates: AP=+0.5 mm, ML=+1.75 mm, DV= −3.5 mm). After 2 wk of recovery, mice were habituated for a week to the recording environment and subsequently connected to a digital Lynx (10S) acquisition system through an HS-16 headstage preamplifier (Neuralynx). Signals were amplified, filtered (600–6000 Hz) and data acquired by using Cheetah software (Neuralynx). After a 10-min habituation baseline, striatal neuron firing properties were recorded for 10 min. Tetrodes were lowered by 50-μm increments each day. Tetrode placement was assessed postmortem by hematoxylin staining of striatal sections. Units were isolated by cluster analysis using Offline Sorter software (Plexon) optimizing clusters for J3 statistics with a minimum clustering probability of

p<0.001. Inter-spike intervals (ISI) of clustered waveforms were subsequently analyzed by using MATLAB (MathWorks).

The distributions of Log(ISI) were plotted and the median and mean values calculated. Two main distributions were observed: neurons with large differences between Log(ISI) median and mean values, representing bouts of activity alternated with silent periods; and a second type of neuron with a more continuous firing and closer median and mean values. To classify all recorded units, we used the ratio of the ISI median/mean values. A ratio of 0.3 was considered the cutoff between the two types of MSN firing patterns.

AAV vector generation and delivery

An AAV-Gpr88-TdTomato vector was generated by fusing human *GPR88* to *TdTomato* coding region and inserting it downstream of the CBA promoter; it was made Cre dependent by inserting an polyadenylation signal flanked by loxP sequences between the promoter and *GPR88*. As a control, an AAV with *TdTomato* under control of the Fos promoter was generated. Encapsidation in AAV1 coat serotype was performed as described[55]

For cell culture studies, 1 μl of the virus/well was used. For *in vivo* viral delivery, 4 μl of the virus (0.5 μl/injection site) were stereotactically injected bilaterally in the dorsal striatum at the coordinates ML=±1.50, AV=+1.2, DV= −3.25/3.75 and ML=±2.25, AV=0, DV= −3.25/3.75 from Bregma. Animals recovered for 2 wk before behavioral testing or electrophysiological recordings.

Intracerebral retrobead delivery

Red fluorescent latex beads (Retrobeads™, Lumafluor; 300 μl) were injected unilaterally in the SNr at the coordinates ML=+1.50, AV= −3.08, DV= −4.75 and ML=+1.50, AV= −3.45, DV= −4.50. Green fluorescent beads (300 μl) were injected unilaterally in the GPe at the coordinates ML= −2.00, AV= −0.58, DV= −4.00. Animals recovered for 2 wk before obtaining slices for recording.

Statistical analyses

Data are shown as the means±s.e.m. GraphPad Prism v5.0 software was used for statistical analyses. For normally-distributed parameters, either Student's t-test (two-group comparisons) or ANOVA tests (multiple comparisons) were used. Otherwise, non-parametrical tests were used. For *in vivo* recordings and microarray analysis, builtin packages were used.

Supplementary Material

Refer to Web version on PubMed Central for supplementary material.

Acknowledgments

This work was supported by grants from NIH NS052536, NS060803, HD02274 (N.S.B.), MH086386 (G.S.M and P.S.A), DA007278 (G.P.S) and GM032875 (G.S.M). A.Q. and E.S. were recipients of MICINN postdoctoral mobility program fellowships. The authors thank Glenda Froelick for assistance with histology, Jones Parker for

help making the targeting construct, Larry Zweifel and Matt Carter for helpful discussions and Diane Durnam for editing.

References

1. Gerfen CR. The neostriatal mosaic: multiple levels of compartmental organization in the basal ganglia. Annu Rev Neurosci. 1992; 15:285–320. [PubMed: 1575444]
2. Surmeier DJ, Plotkin J, Shen W. Dopamine and synaptic plasticity in dorsal striatal circuits controlling action selection. Curr Opin Neurobiol. 2009; 19:621–628. [PubMed: 19896832]
3. Balleine BW, Delgado MR, Hikosaka O. The role of the dorsal striatum in reward and decision-making. J Neurosci. 2007; 27:8161–8165. [PubMed: 17670959]
4. Drew MR, et al. Transient overexpression of striatal D2 receptors impairs operant motivation and interval timing. J Neurosci. 2007; 27:7731–7739. [PubMed: 17634367]
5. Russell VA. Neurobiology of animal models of attention-deficit hyperactivity disorder. J Neurosci Methods. 2007; 161:185–198. [PubMed: 17275916]
6. Graybiel AM, Aosaki T, Flaherty AW, Kimura M. The basal ganglia and adaptive motor control. Science. 1994; 265:1826–1831. [PubMed: 8091209]
7. Joshi PR, et al. Age-dependent alterations of corticostriatal activity in the YAC128 mouse model of Huntington disease. J Neurosci. 2009; 29:2414–2427. [PubMed: 19244517]
8. Massart R, Guilloux JP, Mignon V, Sokoloff P, Diaz J. Striatal GPR88 expression is confined to the whole projection neuron population and is regulated by dopaminergic and glutamatergic afferents. Eur J Neurosci. 2009; 30:397–414. [PubMed: 19656174]
9. Boehm C, et al. Effects of antidepressant treatment on gene expression profile in mouse brain: cell type-specific transcription profiling using laser microdissection and microarray analysis. J Neurochem. 2006; 97 (Suppl 1):44–49.
10. Conti B, et al. Region-specific transcriptional changes following the three antidepressant treatments electro convulsive therapy, sleep deprivation and fluoxetine. Mol Psychiatry. 2007; 12:167–189. [PubMed: 17033635]
11. Befort K, et al. Mu-opioid receptor activation induces transcriptional plasticity in the central extended amygdala. Eur J Neurosci. 2008; 27:2973–2984. [PubMed: 18588537]
12. Logue SF, et al. The orphan GPCR, GPR88, modulates function of the striatal dopamine system: a possible therapeutic target for psychiatric disorders? Mol Cell Neurosci. 2009; 42:438–447. [PubMed: 19796684]
13. Madisen L, et al. A robust and high-throughput Cre reporting and characterization system for the whole mouse brain. Nat Neurosci. 2010; 13:133–140. [PubMed: 20023653]
14. Sanz E, et al. Cell-type-specific isolation of ribosome-associated mRNA from complex tissues. Proc Natl Acad Sci U S A. 2009; 106:13939–13944. [PubMed: 19666516]
15. Darvas M, Palmiter RD. Restricting dopaminergic signaling to either dorsolateral or medial striatum facilitates cognition. J Neurosci. 2010; 30:1158–1165. [PubMed: 20089924]
16. McDonald RJ, White NM. Parallel information processing in the water maze: evidence for independent memory systems involving dorsal striatum and hippocampus. Behav Neural Biol. 1994; 61:260–270. [PubMed: 8067981]
17. Packard MG, Knowlton BJ. Learning and memory functions of the Basal Ganglia. Annu Rev Neurosci. 2002; 25:563–593. [PubMed: 12052921]
18. Darvas M, Palmiter RD. Contributions of striatal dopamine signaling to the modulation of cognitive flexibility. Biol Psychiatry. 2011; 69:704–707. [PubMed: 21074144]
19. van der Heyden JA, Bradford LD. A rapidly acquired one-way conditioned avoidance procedure in rats as a primary screening test for antipsychotics: influence of shock intensity on avoidance performance. Behav Brain Res. 1988; 31:61–67. [PubMed: 2906543]
20. Berke JD, Okatan M, Skurski J, Eichenbaum HB. Oscillatory entrainment of striatal neurons in freely moving rats. Neuron. 2004; 43:883–896. [PubMed: 15363398]
21. Wilson CJ, Kawaguchi Y. The origins of two-state spontaneous membrane potential fluctuations of neostriatal spiny neurons. J Neurosci. 1996; 16:2397–2410. [PubMed: 8601819]

22. Nunez-Abades PA, Pattillo JM, Hodgson TM, Cameron WE. Role of synaptic inputs in determining input resistance of developing brain stem motoneurons. J Neurophysiol. 2000; 84:2317–2329. [PubMed: 11067975]
23. Kravitz AV, et al. Regulation of parkinsonian motor behaviours by optogenetic control of basal ganglia circuitry. Nature. 2010; 466:622–626. [PubMed: 20613723]
24. Ferguson SM, Neumaier JF. Grateful DREADDs: engineered receptors reveal how neural circuits regulate behavior. Neuropsychopharmacology. 2012; 37:296–297. [PubMed: 22157861]
25. Lobo MK, et al. Cell type-specific loss of BDNF signaling mimics optogenetic control of cocaine reward. Science. 2010; 330:385–390. [PubMed: 20947769]
26. Wang W, et al. Regulation of prefrontal excitatory neurotransmission by dopamine in the nucleus accumbens core. J Physiol. 2012; 590:3743–3769. [PubMed: 22586226]
27. Zhang F, et al. Association analyses of the interaction between the ADSS and ATM genes with schizophrenia in a Chinese population. BMC Med Genet. 2008; 9:119. [PubMed: 19115993]
28. Chen X, et al. FBXL21 association with schizophrenia in Irish family and case-control samples. Am J Med Genet B Neuropsychiatr Genet. 2008; 147B:1231–1237. [PubMed: 18404645]
29. Chowdari KV, et al. Association and linkage analyses of RGS4 polymorphisms in schizophrenia. Hum Mol Genet. 2002; 11:1373–1380. [PubMed: 12023979]
30. Berman DM, Wilkie TM, Gilman AG. GAIP and RGS4 are GTPase-activating proteins for the Gi subfamily of G protein alpha subunits. Cell. 1996; 86:445–452. [PubMed: 8756726]
31. Ding J, et al. RGS4-dependent attenuation of M4 autoreceptor function in striatal cholinergic interneurons following dopamine depletion. Nat Neurosci. 2006; 9:832–842. [PubMed: 16699510]
32. Corvin AP, et al. Confirmation and refinement of an ‘at-risk’ haplotype for schizophrenia suggests the EST cluster, Hs.97362, as a potential susceptibility gene at the Neuregulin-1 locus. Mol Psychiatry. 2004; 9:208–213. [PubMed: 14966480]
33. Lerner TN, Kreitzer AC. RGS4 is required for dopaminergic control of striatal LTD and susceptibility to Parkinsonian motor deficits. Neuron. 2012; 73:347–359. [PubMed: 22284188]
34. Song I, Huganir RL. Regulation of AMPA receptors during synaptic plasticity. Trends Neurosci. 2002; 25:578–588. [PubMed: 12392933]
35. Jacob TC, Moss SJ, Jurd R. GABA(A) receptor trafficking and its role in the dynamic modulation of neuronal inhibition. Nat Rev Neurosci. 2008; 9:331–343. [PubMed: 18382465]
36. Janssen MJ, Ade KK, Fu Z, Vicini S. Dopamine modulation of GABA tonic conductance in striatal output neurons. J Neurosci. 2009; 29:5116–5126. [PubMed: 19386907]
37. Parker JG, et al. Attenuating GABA(A) receptor signaling in dopamine neurons selectively enhances reward learning and alters risk preference in mice. J Neurosci. 2011; 31:17103–17112. [PubMed: 22114279]
38. Ade KK, Janssen MJ, Ortinski PI, Vicini S. Differential tonic GABA conductances in striatal medium spiny neurons. J Neurosci. 2008; 28:1185–1197. [PubMed: 18234896]
39. Farrant M, Nusser Z. Variations on an inhibitory theme: phasic and tonic activation of GABA(A) receptors. Nat Rev Neurosci. 2005; 6:215–229. [PubMed: 15738957]
40. Zweifel LS, et al. Disruption of NMDAR-dependent burst firing by dopamine neurons provides selective assessment of phasic dopamine-dependent behavior. Proc Natl Acad Sci U S A. 2009; 106:7281–7288. [PubMed: 19342487]
41. Nicola SM, Surmeier J, Malenka RC. Dopaminergic modulation of neuronal excitability in the striatum and nucleus accumbens. Annu Rev Neurosci. 2000; 23:185–215. [PubMed: 10845063]
42. Surmeier DJ, et al. The role of dopamine in modulating the structure and function of striatal circuits. Prog Brain Res. 2010; 183:149–167. [PubMed: 20696319]
43. Ralph-Williams RJ, Lehmann-Masten V, Otero-Corchon V, Low MJ, Geyer MA. Differential effects of direct and indirect dopamine agonists on prepulse inhibition: a study in D1 and D2 receptor knock-out mice. J Neurosci. 2002; 22:9604–9611. [PubMed: 12417685]
44. Kodsi MH, Swerdlow NR. Quinolinic acid lesions of the ventral striatum reduce sensorimotor gating of acoustic startle in rats. Brain Res. 1994; 643:59–65. [PubMed: 8032933]

45. Braff DL, Geyer MA, Swerdlow NR. Human studies of prepulse inhibition of startle: normal subjects, patient groups, and pharmacological studies. Psychopharmacology (Berl). 2001; 156:234–258. [PubMed: 11549226]

46. Brandish PE, et al. Regulation of gene expression by lithium and depletion of inositol in slices of adult rat cortex. Neuron. 2005; 45:861–872. [PubMed: 15797548]

47. Ogden CA, et al. Candidate genes, pathways and mechanisms for bipolar (manic-depressive) and related disorders: an expanded convergent functional genomics approach. Mol Psychiatry. 2004; 9:1007–1029. [PubMed: 15314610]

48. Farley FW, Soriano P, Steffen LS, Dymecki SM. Widespread recombinase expression using FLPeR (flipper) mice. Genesis. 2000; 28:106–110. [PubMed: 11105051]

49. Quintana A, Kruse SE, Kapur RP, Sanz E, Palmiter RD. Complex I deficiency due to loss of Ndufs4 in the brain results in progressive encephalopathy resembling Leigh syndrome. Proc Natl Acad Sci U S A. 2010; 107:10996–11001. [PubMed: 20534480]

50. Perez FA, Palmiter RD. Parkin-deficient mice are not a robust model of parkinsonism. Proc Natl Acad Sci U S A. 2005; 102:2174–2179. [PubMed: 15684050]

51. Darvas M, Fadok JP, Palmiter RD. Requirement of dopamine signaling in the amygdala and striatum for learning and maintenance of a conditioned avoidance response. Learn Mem. 2011; 18:136–143. [PubMed: 21325435]

52. Duncan DT, Prodduturi N, Zhang B. WebGestalt2: an updated expanded version of the Web-based Gene Set Analysis Toolkit. Bmc Bioinformatics. 2010; 11:1. [PubMed: 20043860]

53. Ariano MA, et al. Striatal potassium channel dysfunction in Huntington's disease transgenic mice. J Neurophysiol. 2005; 93:2565–2574. [PubMed: 15625098]

54. Mermelstein PG, Song WJ, Tkatch T, Yan Z, Surmeier DJ. Inwardly rectifying potassium (IRK) currents are correlated with IRK subunit expression in rat nucleus accumbens medium spiny neurons. J Neurosci. 1998; 18:6650–6661. [PubMed: 9712637]

55. Quintana A, et al. Fatal breathing dysfunction in a mouse model of Leigh syndrome. J Clin Invest. 2012; 122:2359–2368. [PubMed: 22653057]

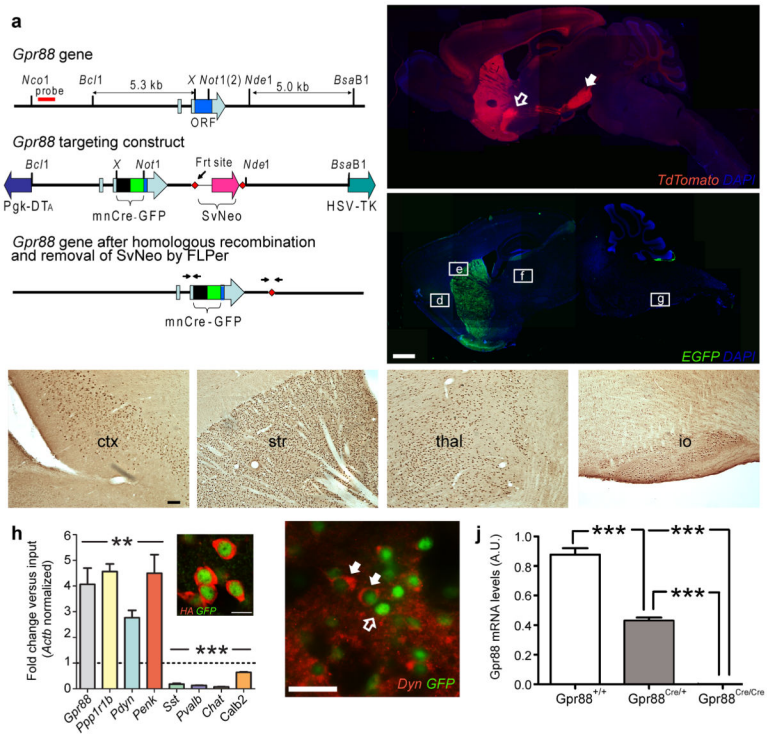

Figure 1. Characterization of Gpr88-Cre-EGFP mice

(**a**) Gene targeting strategy to generate a Gpr88-Cre-EGFP line of mice. (**b**) Composite sagittal image of a Gpr88-Cre-EGFP; TdTomato reporter mouse. Cre-mediated recombination (red) is observed as fluorescence in striatum, olfactory tubercle and cortex. Terminals from striatonigral (filled arrow) and striatopallidal (open arrow) MSNs are visible in the SNr and GPe, respectively. (**c**) Composite sagittal image of EGFP fluorescence in adult Gpr88-Cre-EGFP mice. EGFP-positive cells are observed in the striatum and olfactory tubercle. Scale bar: 1 mm (**d–g**) Immunohistochemistry detected low-level EGFP expression in cortex (ctx), striatum (str), thalamus (thal) and inferior olive (io) of an adult Gpr88-Cre-EGFP mouse; locations shown in (**c**). Bar: 100 μm. (**h**) qRT-PCR analysis of transcripts expressed in Gpr88-Cre-EGFP-expressing neurons after immunoprecipitation of HA-tagged polysomes from Gpr88-Cre-EGFP:RiboTag forebrain slices. MSN-specific mRNAs (*Ppp1r1b*, *Pdyn*, *Penk*) as well as *Gpr88* were enriched in the pellet fraction compared to the input. Striatal interneuron-specific marker mRNAs (*Sst*, *Pvalb*, *Chat*, *Calb2*) were less abundant in the pellet fraction. ***p<0.001; ** p<0.01. Student's t-test, two-tailed (fold=1; dashed line. n=3). H (inset), HA (red), and EGFP (green) double immunofluorescence shows co-localization in the striatum. Bar: 12.5 μm. (**i**) Double immunofluorescence against dynorphin (Dyn; red) and EGFP (green). Both Dyn and EGFP double-positive cells (filled arrows) and Dyn negative but EGFP-positive cells (open arrow) were observed in the striatum of $Gpr88^{Cre/+}$ mice. Bar: 50 μm. (**j**) qRT-PCR analysis of *Gpr88* mRNA in $Gpr88^{+/+}$, $Gpr88^{Cre/+}$ and $Gpr88^{Cre/Cre}$ mice (n=3 each). ***p<0.001, one-way ANOVA, SNK post-test. Values are shown as mean ± s.e.m.

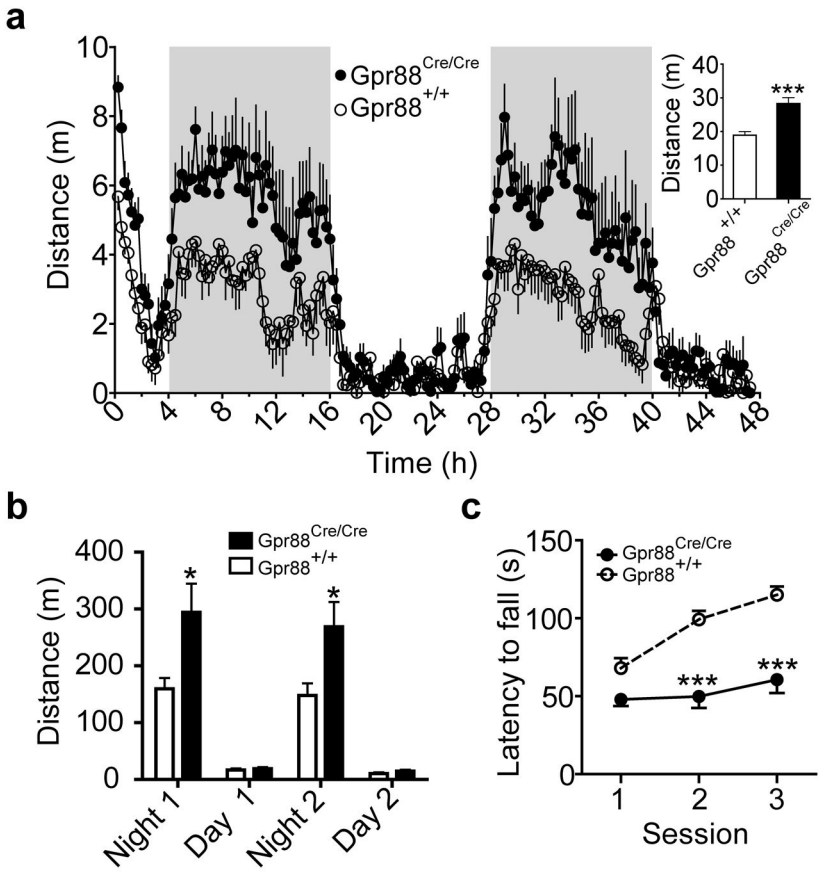

Figure 2. Hyperlocomotion and motor deficits in *Gpr88*$^{Cre/Cre}$ mice

(**a**) Locomotion (48 h) of *Gpr88*$^{+/+}$ (n=9) and *Gpr88*$^{Cre/Cre}$ (n=12) mice. Animals were placed in a novel chamber and their activity was acquired in 15-min bins. (inset) Novelty-induced locomotion (1 h) in *Gpr88*$^{+/+}$ and *Gpr88*$^{Cre/Cre}$ mice. ***p<0.001 Student's t-test versus *Gpr88*$^{+/+}$, two-tailed. (**b**) Diurnal and nocturnal locomotion in *Gpr88*$^{+/+}$ and *Gpr88*$^{Cre/Cre}$ mice. *p<0.05., genotype, rmANOVA, Bonferroni post-test. (**c**) Rotarod performance by *Gpr88*$^{+/+}$ (n=15) and *Gpr88*$^{Cre/Cre}$ (n=14) mice. Animals were placed in an accelerating rotating rod (4 to 40 rpm) for 3 min and the latency to fall was recorded. ***p<0.001, genotype, rmANOVA, Bonferroni post-test. Values are shown as mean ± s.e.m.

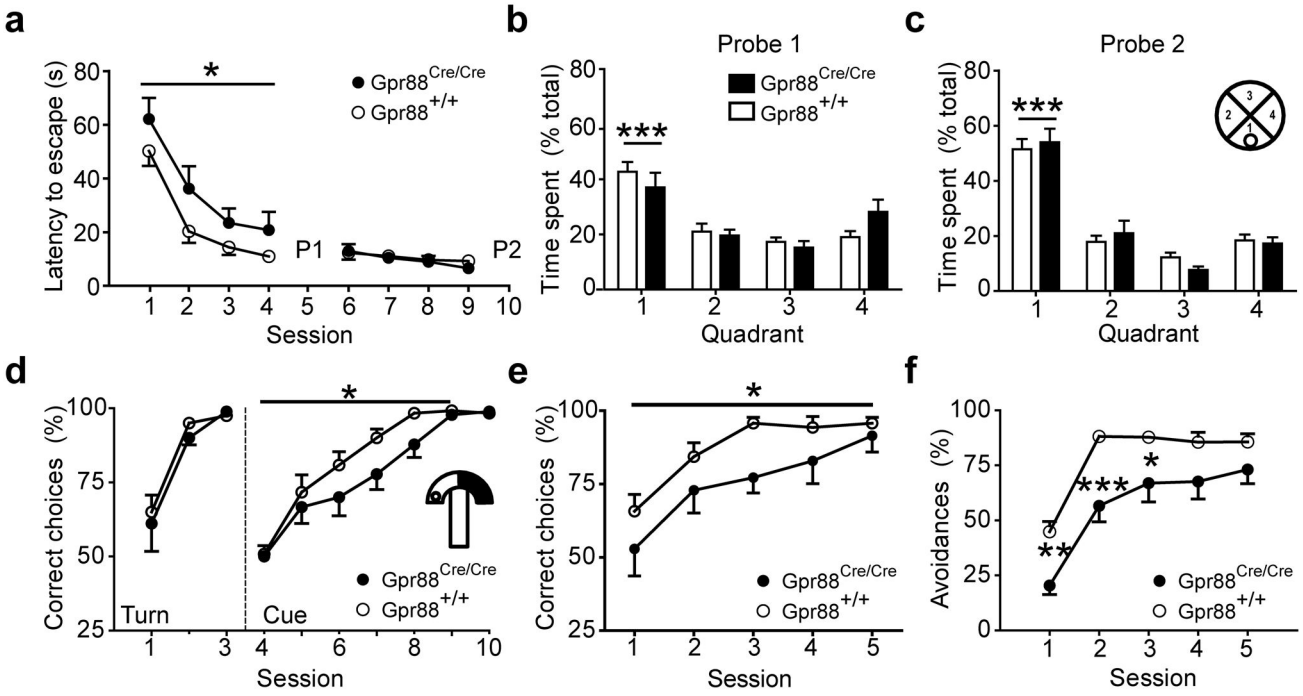

Figure 3. Impaired cue-based learning by *Gpr88*$^{Cre/Cre}$ mice

(**a–c**) Morris water maze performance by *Gpr88*$^{+/+}$ (n=12) and *Gpr88*$^{Cre/Cre}$ (n=9) mice. Animals were trained for 4 d (2 trials/d) to find a hidden platform and the latency to escape was recorded (**a**; *p<0.05, genotype, rmANOVA). On day 5, a probe trial (P1) was performed and the time *Gpr88*$^{+/+}$ and *Gpr88*$^{Cre/Cre}$ mice spent in the target quadrant (**c**; inset) was recorded (**b**). Then mice received 4 more training sessions (**a**) and then another probe trial (P2) was performed (**c**; ***p<0.001, quadrant, rmANOVA, Bonferroni post-test). (**d**) Water U-maze performance by *Gpr88*$^{+/+}$ (n=12) and *Gpr88*$^{Cre/Cre}$ (n=9) mice. Animals were trained on a turn-based escape paradigm for 3 d (10 trials/d) to find a platform placed in one arm of the maze (inset). Correct choices (*p<0.05, genotype, rmANOVA Bonferroni post-test) were recorded. On day 4, animals were forced to shift to cue-based learning (as platform was associated with an arm color) and correct choices were recorded. (**e**) *Gpr88*$^{+/+}$ (n=7) and *Gpr88*$^{Cre/Cre}$ (n=7) mice were trained only on a cue-based learning paradigm and the percentage of correct choices was recorded. (*p<0.05, genotype, rmANOVA). (**f**) Two-way active avoidance test with *Gpr88*$^{+/+}$ (n=14) and *Gpr88*$^{Cre/Cre}$ (n=10) mice. *p<0.05, **p<0.01, ***p<0.001, genotype, rmANOVA, Bonferroni post-test. Values are shown as mean ± s.e.m.

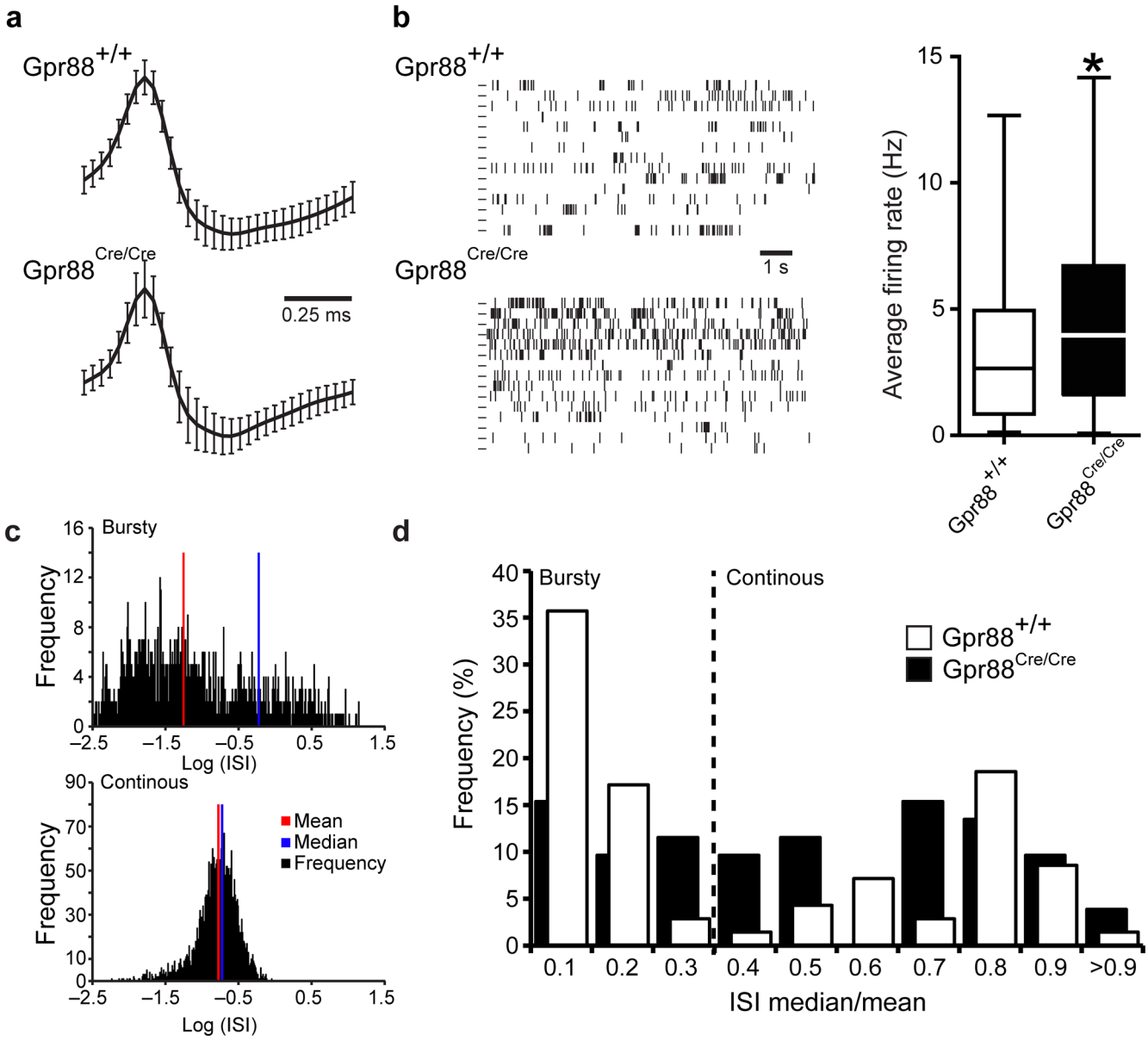

Figure 4. Increased firing rate in MSNs of freely moving *Gpr88*$^{Cre/Cre}$ mice

(**a–c**) Electrophysiological recordings of MSNs *in vivo*. (**a**) Putative MSNs had waveforms >300 μs valley width. (**b**) (left panel) Raster plots of 15 representative MSNs from *Gpr88*$^{+/+}$ and *Gpr88*$^{Cre/Cre}$ mice. (right panel). Increased average firing rate in MSN of *Gpr88*$^{Cre/Cre}$ mice (n=52 units, 6 mice) compared to *Gpr88*$^{+/+}$ mice (n=70 units, 6 mice). *p<0.05, Student's t-test versus *Gpr88*$^{+/+}$, two-tailed. (**c**) Representative MSN firing frequencies of a bursty-type MSN and a continuously firing MSN. (**d**) Continuous firing was more frequent in MSNs from *Gpr88*$^{Cre/Cre}$ mice (p<0.05, Fisher's exact test, two-tailed). Values are shown as mean ± s.e.m.

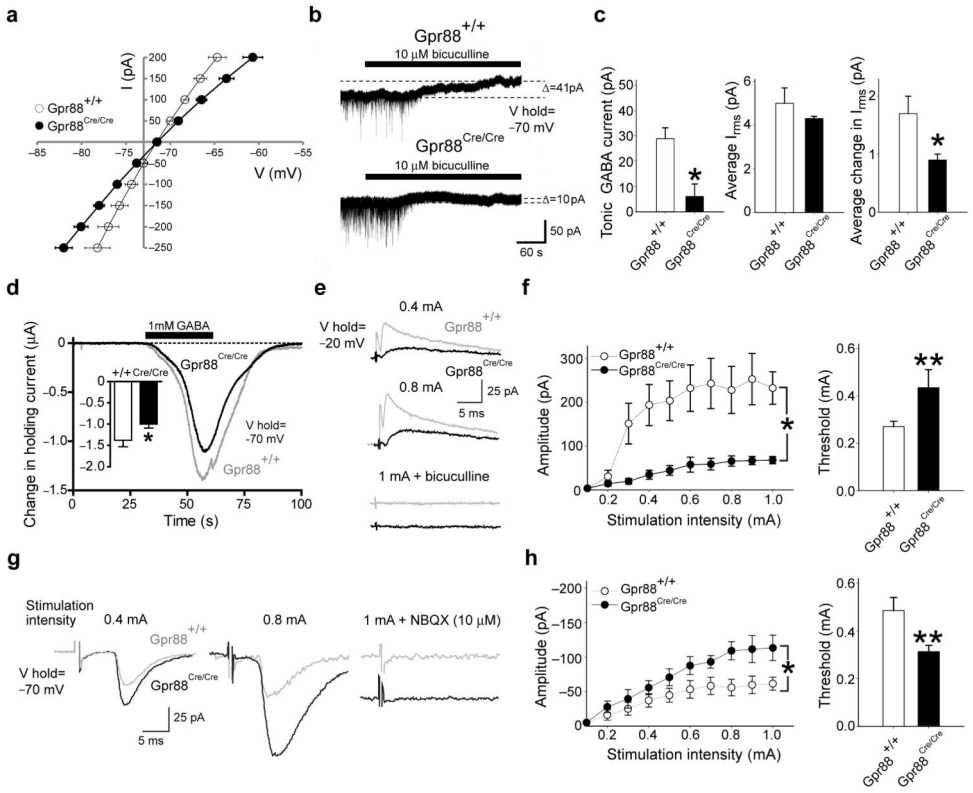

Figure 5. Reduced GABAergic and enhanced glutamatergic signaling in MSNs of *Gpr88*$^{Cre/Cre}$ mice

(**a**) Current-voltage (I–V) curves in response −250 to +200 pA inputs (p<0.001, nonlinear fit) in *Gpr88*$^{+/+}$ (n=16 cells) and *Gpr88*$^{Cre/Cre}$ mice (n=18 cells). (**b**) Representative traces show bicuculline-sensitive tonic currents in MSNs (held at −70 mV). (**c**) Mean tonic GABA current (left), mean baseline I_{rms} (middle), and the average change in I_{rms} following bicuculline (right). *p<0.05, Student's t-test, two-tailed in *Gpr88*$^{+/+}$ (n=8 cells) and *Gpr88*$^{Cre/Cre}$ (n=10 cells) mice. (**d**) Representative traces and peak GABA current (μA; inset) in response to GABA. *p<0.05, Student's t-test (n=9 cells each). (**e**) Representative traces in cells from *Gpr88*$^{+/+}$ and *Gpr88*$^{Cre/Cre}$ mice showing evoked IPSCs in response to intrastriatal stimulation, and following bicuculline. (**f**) (left panel) Mean peak outward current responses in cells from *Gpr88*$^{+/+}$ (n=15 cells) and *Gpr88*$^{Cre/Cre}$ (n=17 cells) mice. *p<0.05 Two-way ANOVA (right panel) Average stimulation current required to reach threshold in *Gpr88*$^{+/+}$ and *Gpr88*$^{Cre/Cre}$ cells. **p<0.01 Student's t-test, two-tailed. (**g**) Representative traces showing evoked EPSCs in MSNs from *Gpr88*$^{Cre/Cre}$ and *Gpr88*$^{+/+}$ mice. The AMPA receptor antagonist NBQX prevented the evoked current. (**h**) (left panel) Mean peak current evoked by increasing stimulation intensity (*p<0.05 two-way ANOVA) and (right panel) the average stimulation current required to reach threshold. **p<0.01, Student's t-test, two-tailed. Values are shown as mean ± s.e.m.

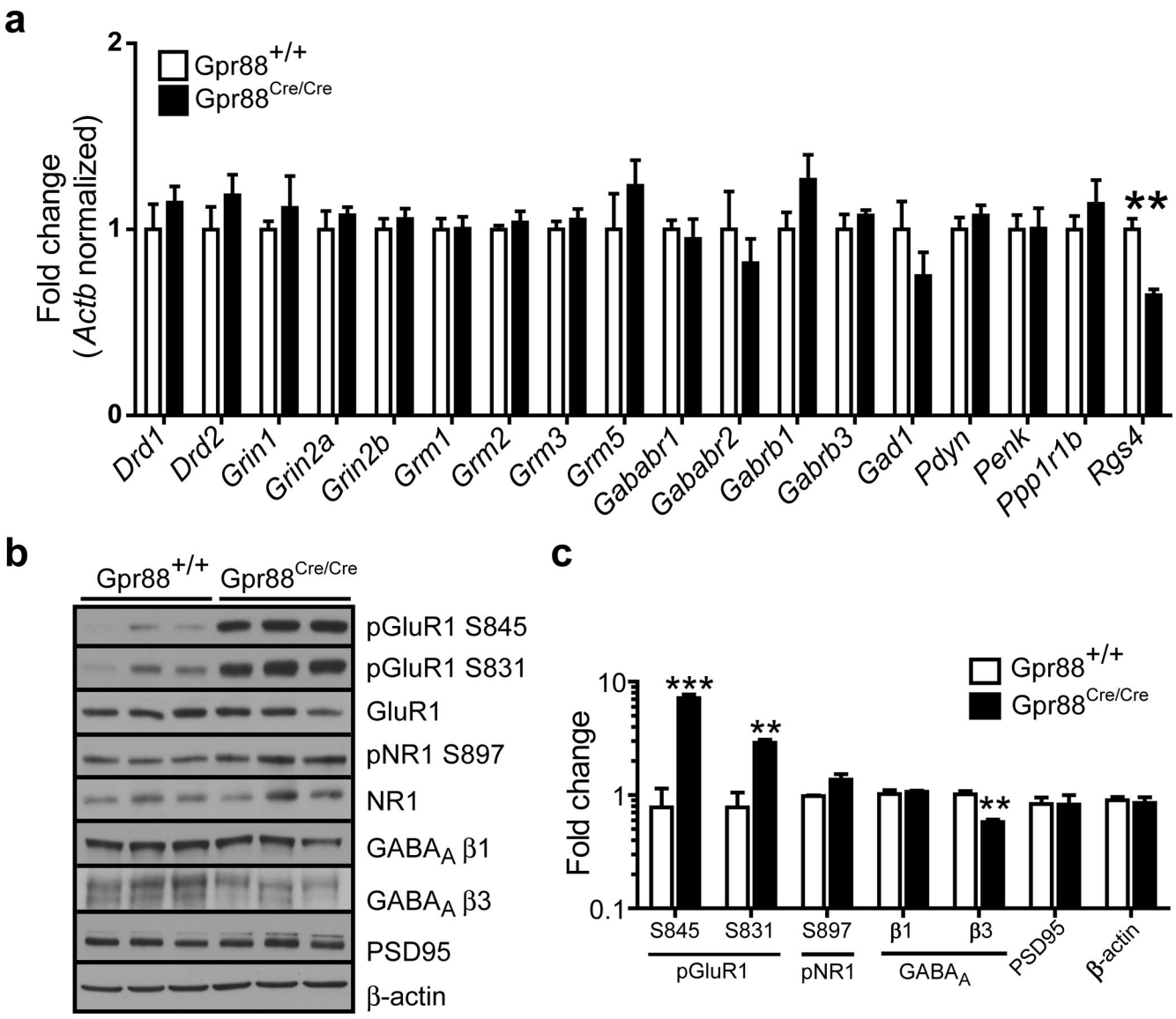

Figure 6. Alterations in mRNA and intracellular signaling in striatum of *Gpr88*$^{Cre/Cre}$ mice

(a) qRT-PCR analysis of neurotransmitter receptors/subunits: dopaminergic (*Drd1*, *Drd2*), glutamatergic (*Grin1, Grin2a, Grin2b, Grm1, Grm2, Grm3, Grm5*) and GABAergic (*Gababr1, Gababr2, Gababrb1, Gababrb3, Gad1*), and molecules involved in intracellular signaling cascades (*Ppp1r1b, Pdyn, Penk, Rgs4*) in whole striata from *Gpr88*$^{+/+}$ (n=4) and *Gpr88*$^{Cre/Cre}$ (n=4–6) mice. All genes were normalized to beta-actin (*Actb*) levels using the ΔΔCt method. ** p<0.01 Student's t-test, two-tailed, versus *Gpr88*$^{+/+}$. (**b,c**) Representative western blot analysis (**b**) and quantification (**c**) of total and phosphorylated NR1 (Ser897) and GluR1 (Ser845, Ser831,) glutamate receptor subunits, total GABA-$_A$ receptor β1 and β3 subunits and PSD95 and β-actin in striatal samples from *Gpr88*$^{+/+}$ and *Gpr88*$^{Cre/Cre}$ mice (n=3 of each genotype, 3 independent experiments). Optical densities were determined and normalized to β-actin. For phosphorylated residues, the fold change denotes the

phosphorylated versus total normalized values. **p<0.01, ***p<0.001 Student's t-test, two-tailed. Values are shown as mean ± s.e.m.

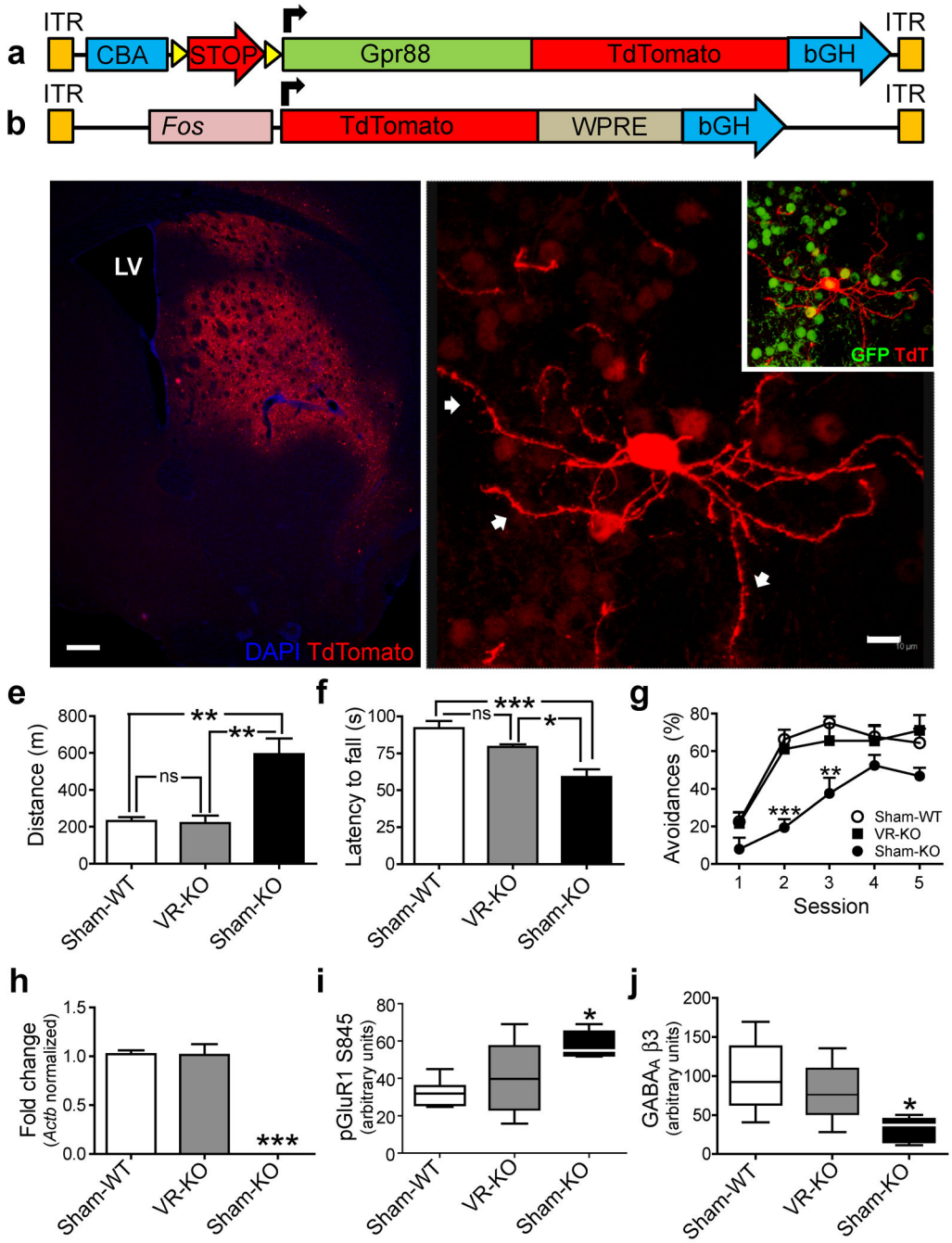

Figure 7. Viral re-expression of GPR88 in striatum restores the molecular properties and behavior

(**a,b**) Schematic representation of the AAV-based viral vectors used for striatal GPR88 restoration: (**a**), floxed-STOP AAV-CBA-GPR88-TdTomato (loxP sites represented as yellow triangles) and (**b**) AAV-Fos-TdTomato (control). (**c**) Representative anti-TdTomato immunofluorescence in a striatal section of a virally-rescued *Gpr88*$^{Cre/Cre}$ (VR-KO) mouse. LV: Lateral Ventricle. Scale bar: 250 μm. (**d**) High-magnification confocal image of a transduced cell in a VR-KO mouse showing presence of the GPR88-TdTomato fusion

protein throughout the cell, dendrites, and spines (arrows). Co-localization with EGFP shows that it is a MSN (**d**, inset). Bar: 10 μm. (**e**) Locomotor activity (48 h) of Sham-WT (n=15), VR-KO (n=7) and Sham-KO (n=9) mice. **p<0.01, Kruskall-Wallys test, Dunn post-test (**f**) Rotarod performance (last session) of Sham-WT (n=18), VR-KO (n=8) and Sham-KO (n=11) mice. *p<0.05, ***p<0.001, one-way ANOVA, SNK post-test. (**g**) Two-way active avoidance performance of Sham-WT (n=10), VR-KO (n=8) and Sham-KO (n=5) mice. **p<0.01, ***p<0.001, genotype, rmANOVA, Bonferroni post-test. (**h**) qRT-PCR analysis of *Gpr88* in striatum of Sham-WT, VR-KO and Sham-KO mice (n=4 Sham-WT, Sham-KO; n=6 VR-KO). Results were normalized to beta-actin (*Actb*) levels using the ΔΔCt method. ***p<0.001, one-way ANOVA, SNK post-test. (**i,j**) Western blot analysis of GluR1 S845 phosphorylation (**i**) or GABA-A receptor β3 (**j**) in striatum of Sham-WT, VR-KO and Sham-KO mice (n=6 each). Results were normalized to β-actin levels. *p<0.05 one-way ANOVA, SNK post-test. Values are shown as mean ± s.e.m.

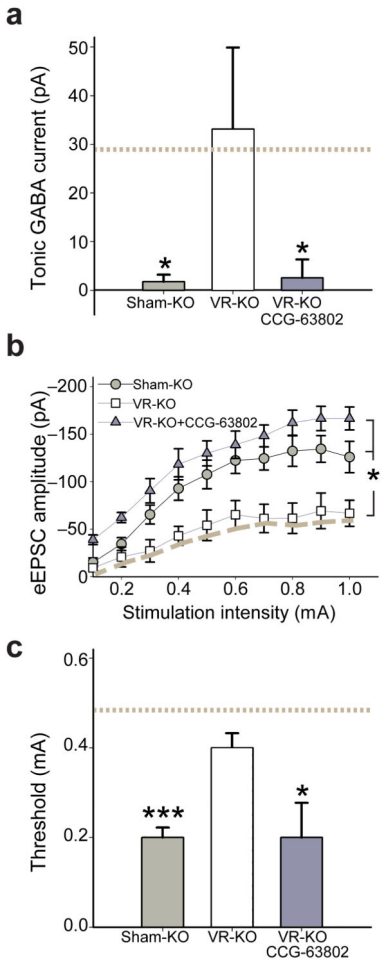

Figure 8. Intracellular RGS4 activity in MSNs is required for viral-mediated electrophysiological rescue

(**a**) Mean tonic GABA current following bicuculline in MSNs from Sham-KO (n=12 cells, 3 mice) and VR-KO (n=7 cells, 3 mice) mice and in VR-KO mice 15 min following patch pipette dialysis of the RGS4 inhibitor CCG-63802 (n=4). *p<0.05, Student's t-test versus VR-KO. Gray line denotes *Gpr88*$^{+/+}$ values (from Fig. 5c) as reference. (**b**) Mean peak current evoked by increasing stimulation intensity (*p<0.05, genotype, 2-way ANOVA), and (**c**) the average stimulation current required to reach threshold in MSNs from Sham-KO (n=16, 3 mice), VR-KO (n=11 cells, 3 mice) mice and in cells from VR-KO mice that were infused with the RGS4 inhibitor CCG-63802 (n=5 cells, 3 mice). *p<0.05, ***p<0.001, Student's t-test versus VR-KO. Gray lines denote *Gpr88*$^{+/+}$ values (from Fig. 5h) as reference. Values are shown as mean ± s.e.m.